

# An Infrared Study of $\pi$ -Hydrogen Bonds in Micro-solvated Phenol: OH Stretching Vibrations of Phenol–X (X = C<sub>6</sub>H<sub>6</sub>, C<sub>2</sub>H<sub>4</sub>, and C<sub>2</sub>H<sub>2</sub>) Clusters in the Neutral and Cationic Ground States

Asuka Fujii,\* Takayuki Ebata, and Naohiko Mikami\*

Department of Chemistry, Graduate School of Sciences, Tohoku University, Sendai 980-8578, Japan

Received: April 3, 2002; In Final Form: July 2, 2002

Infrared spectra of phenol–X (X = C<sub>6</sub>H<sub>6</sub>, C<sub>2</sub>H<sub>4</sub>, and C<sub>2</sub>H<sub>2</sub>) clusters in the neutral and cationic ground states were observed in the OH stretching vibrational region. For the neutral ground state, infrared–ultraviolet double resonance spectroscopy was utilized to observe the infrared spectra. A small low-frequency shift of the OH vibration of the phenol site in all the clusters represented the characteristic feature for their  $\pi$ -hydrogen-bonded structures, which were also confirmed by density functional theoretical calculations. The OH frequency shifts did not remarkably depend on the type of the  $\pi$ -electrons. The correlation between the proton affinity of X and the OH frequency shift, which has been known for conventional  $\sigma$ -hydrogen-bonded phenol clusters, was held in phenol–C<sub>2</sub>H<sub>4</sub> and –C<sub>2</sub>H<sub>2</sub>, while phenol–C<sub>6</sub>H<sub>6</sub> showed a clear deviation from the correlation. For the cationic ground state, infrared photodissociation spectroscopy was used to observe the infrared spectra. The OH frequency of these clusters exhibited an extremely large low-frequency shift upon ionization, reflecting the significant enhancement of the  $\pi$ -hydrogen bond strength. The  $\pi$ -hydrogen bond energies in the cations were estimated on the basis of both the experiments and the theoretical calculations.

## I. Introduction

It is well-known that  $\pi$ -electrons in a molecule exhibit weak proton acceptability, and act as a proton acceptor for hydrogen bonding.<sup>1,2</sup> Such a hydrogen bond is classified as “ $\pi$ -hydrogen bond”, and is generally categorized as a weak hydrogen bond. Their binding energies are estimated to be lower than 5 kcal/mol, and these values are much smaller than those of typical  $\sigma$ -hydrogen bonds (5–15 kcal/mol), which are formed between a lone pair of electrons of an electronegative atom and a proton donor. Though the binding energy of  $\pi$ -hydrogen bonds is generally quite small, it has been pointed out that  $\pi$ -hydrogen bonds are of potential importance in structure and function of biological macromolecules. Such a weak  $\pi$ -hydrogen bond is easily perturbed by the environment of the system, so that not so many details of its intrinsic nature are known. In this respect, isolated molecular clusters produced in a supersonic jet provide us with more precise information for the characterization of its nature. Moreover, molecular clusters enable us to study  $\pi$ -hydrogen bonds in cationic systems. Most of our knowledge on  $\pi$ -hydrogen bonds is concerned with the neutral state, and  $\pi$ -hydrogen bonds in the cationic systems have scarcely been studied. Because a charge created in a cluster upon ionization induces substantial electrostatic and inductive interactions, a remarkable enhancement of the hydrogen bond strength is expected for the cationic state of a  $\pi$ -hydrogen-bonded system. Such a phenomenon has scarcely been observed in the condensed phases because of coexisting neutral species that may interfere with the inherent nature of the cations. On the other hand, in the case of a cluster study, the interference can be eliminated in a supersonic jet expansion, although spectroscopy must be carried out by using special techniques.<sup>3–5</sup>

Clusters involving phenol have been extensively studied as typical examples of hydrogen-bonded clusters.<sup>4,6,7</sup> Among them,

phenol–benzene can be regarded as a prototype of  $\pi$ -hydrogen-bonded systems. This cluster was observed by Abe et al. for the first time in an electronic spectroscopic study.<sup>8</sup> Hartland et al. applied ionization-detected stimulated Raman spectroscopy to observe the OH stretching vibrations of the phenol site of the cluster.<sup>9</sup> The OH frequency showed a low-frequency shift of 78 cm<sup>–1</sup> due to the cluster formation, and it offers evidence for the  $\pi$ -hydrogen-bonded structure of the cluster, in which phenol donates the proton to the  $\pi$ -electrons of benzene. A time-resolved photofragment detection study by Knee et al. showed that the binding energy of phenol–benzene in the neutral ground state (S<sub>0</sub>) is in the range of 1250–1550 cm<sup>–1</sup>.<sup>10</sup> On the other hand, in our previous study, we observed the OH stretching vibration of phenol–benzene in the cationic ground state (D<sub>0</sub>) by using infrared (IR) photodissociation spectroscopy.<sup>11</sup> In the cluster cation, the OH frequency shift due to the  $\pi$ -hydrogen bond was found to be over 470 cm<sup>–1</sup>. This extremely large frequency shift of the cation is six times larger than that in the neutral, and such a large shift clearly demonstrates a significant enhancement of the  $\pi$ -hydrogen bond strength upon ionization.

In the present paper, we report an IR spectroscopic study of  $\pi$ -hydrogen-bonded clusters of phenol with hydrocarbons, which possess three different types of  $\pi$ -electrons. The phenol–benzene cluster is revisited as a prototype of the aromatic  $\pi$ -electrons. Phenol–ethylene and –acetylene clusters are studied as examples of the  $\pi$ -electrons in the unsaturated double and triple bonds, respectively. The OH stretching vibrations of the phenol site in these clusters are observed both in S<sub>0</sub> and in D<sub>0</sub>. The  $\pi$ -hydrogen bond strength of the clusters and its enhancement associated with ionization are discussed.

## II. Experimental Section

In this study, the OH stretching vibrations of the phenol–benzene, –ethylene, and –acetylene clusters in the S<sub>0</sub> and D<sub>0</sub> states were observed under molecular beam conditions. The

\* Authors to whom correspondence should be addressed.

infrared–ultraviolet (IR–UV) double resonance technique was used for IR spectroscopy in  $S_0$ , while IR spectra in  $D_0$  were obtained by using infrared photodissociation (IRPD) spectroscopy. Each technique was described elsewhere in detail.<sup>4,12</sup> Here we give only a brief description for each method.

**(A) IR–UV Double Resonance Spectroscopy for the Neutral Ground State.** A pulsed UV laser of which wavelength is fixed at the origin band of the  $S_1$ – $S_0$  transition of the cluster is introduced, and the resonance-enhanced multiphoton ionization (REMPI) signal is observed as a measure of the ground-state population. Prior to the UV laser, an IR laser pulse is introduced, and its wavelength is scanned. When the IR wavelength is resonant with a vibrational transition of the cluster, the IR absorption induces a reduction of the ground-state population, which is detected as a decrease of the REMPI signal intensity.

**(B) IRPD Spectroscopy for Cluster Cations.** The cluster cation was produced by REMPI of the corresponding neutral cluster via its vibrational ground level of  $S_1$ . The IR laser is introduced after a delay time of 50 ns from the ionization. When the IR wavelength is resonant with a vibrational transition of the cluster ion, the vibrational excitation causes vibrational predissociation of the cluster ion, leading to a depletion of the cluster ion intensity. Thus, by scanning the IR wavelength while monitoring the cluster ion intensity, the IR spectrum of the cluster ion is obtained as a depletion spectrum.

The sample of phenol is kept at the room temperature, and its vapor is seeded in a He/Ar/hydrocarbon mixture carrier gas of 4 atm stagnation pressure. The concentration of the solvent hydrocarbon in the mixture gas is 5, 10, and 5% for the production of phenol–benzene, –ethylene, and –acetylene, respectively. The gaseous mixture is expanded into a vacuum chamber through a pulsed valve. Typical background pressure of the chamber is  $6 \times 10^{-6}$  and  $8 \times 10^{-7}$  Torr with and without the valve operation, respectively. The jet expansion is skimmed by a skimmer of 2 mm diameter, and the resultant molecular beam is introduced into the interaction region. A time-of-flight mass spectrometer is used for the mass-separation of ions.

### III. Results and Discussion

**A.  $\pi$ -Hydrogen Bonds in the Neutral Ground State. 1. IR Spectra in the OH Stretching Vibrational Region.** Figure 1 shows the OH stretching vibrational region of IR spectra in  $S_0$  for (a) bare phenol, (b) phenol–benzene, (c) phenol–ethylene, and (d) phenol–acetylene, respectively. Each spectrum is obtained by monitoring the REMPI signal due to the excitation of the  $S_1$ – $S_0$  origin band while scanning the IR wavelength. The origin band positions of the  $S_1$ – $S_0$  electronic spectra are 36348, 36203, 36086, and 36102  $\text{cm}^{-1}$  for bare phenol, phenol–benzene, phenol–ethylene, and phenol–acetylene, respectively. The OH band of bare phenol appears at 3657  $\text{cm}^{-1}$ , while those of the phenol site in the clusters are found at 3579, 3580, and 3589  $\text{cm}^{-1}$  for phenol–benzene, phenol–ethylene, and phenol–acetylene, respectively. The OH frequency of phenol–benzene agrees well with the previously reported value obtained by ionization-detected stimulated Raman spectroscopy.<sup>9</sup> The OH frequency shifts due to the cluster formation are  $-78$ ,  $-77$ , and  $-68$   $\text{cm}^{-1}$ , for phenol–benzene, phenol–ethylene, and phenol–acetylene, respectively. These low-frequency shifts of the OH band indicate that the hydroxyl group of the phenol moiety is hydrogen-donating to the  $\pi$ -electron cloud of the hydrocarbon moiety because the  $\pi$ -electrons are the unique proton acceptor site in these hydrocarbons. The OH frequency shifts of these clusters are much smaller than those of typical  $\sigma$ -hydrogen-

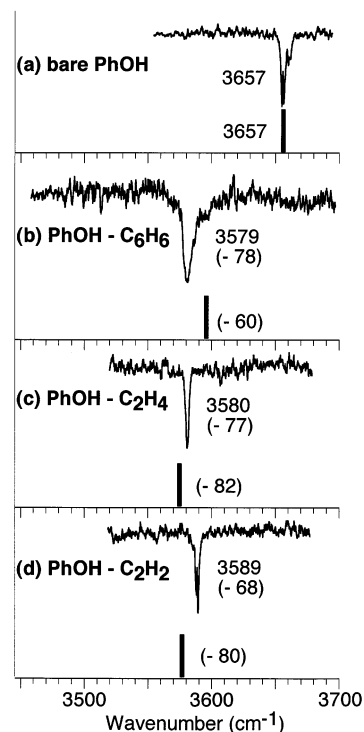


**Figure 1.** OH stretching vibrational region of infrared (IR) spectra of (a) bare phenol (PhOH), (b) phenol–benzene, (c) phenol–ethylene, and (d) phenol–acetylene in the neutral ground state ( $S_0$ ). Infrared–ultraviolet double resonance spectroscopy is used to record the spectra. Bar graphs below the observed spectra indicate the calculated OH frequencies at the B3LYP/6-31G(d, p) level. The scaling factor of 0.9566 is applied to all the calculated frequencies. Numbers in the parentheses are the OH frequency shifts due to the cluster formation.

bonded clusters of phenol with proton acceptors such as water ( $-133$   $\text{cm}^{-1}$ ), methanol ( $-201$   $\text{cm}^{-1}$ ), ammonia ( $-363$   $\text{cm}^{-1}$ ), and trimethylamine ( $-590$   $\text{cm}^{-1}$ ), in which the OH is bound to the lone pair of the acceptors.<sup>13</sup> Since the OH frequency shift can be regarded as a measure of the hydrogen bond strength, much smaller OH frequency shifts in the phenol  $\pi$ -hydrogen-bonded clusters reflect a substantially weaker strength of the  $\pi$ -hydrogen bonds than those of the  $\sigma$ -hydrogen bonds. Since the OH frequency shifts of these three  $\pi$ -hydrogen-bonded clusters fall into a small range within 10  $\text{cm}^{-1}$ , it is suggested that the  $\pi$ -hydrogen bond strength does not significantly depend on the type of the carbon–carbon multiple bonds.

**2. Density Functional Theoretical (DFT) Calculations.** DFT calculations of the phenol–hydrocarbon clusters in their neutral ground state were carried out to confirm the cluster structures inferred by the IR spectra. The Gaussian 98 program package was used to calculate the energy-optimized structures and their harmonic frequencies at the B3LYP/6-31G(d, p) level.<sup>14,15</sup> The minimum energy structures of the clusters calculated at this level are seen in Figure 2.<sup>16</sup> The key structural parameters are also given in Figure 2, and the values in the parentheses are those in the cationic ground state discussed in Section III.B.2. For all the clusters, the  $\pi$ -hydrogen-bonded structures, in which phenol acts as a proton donor to the  $\pi$ -electrons in the hydrocarbon, were actually obtained as their minimum energy structure, as is expected from the IR spectra.

In the case of phenol–benzene, the hydroxyl group is bound on a carbon–carbon bond rather than on the center of the aromatic ring. This structure suggests that the  $\pi$ -hydrogen bond is localized only to a part of the aromatic ring, and the C–H bond at the ortho position of the phenol site is also  $\pi$ -hydrogen-

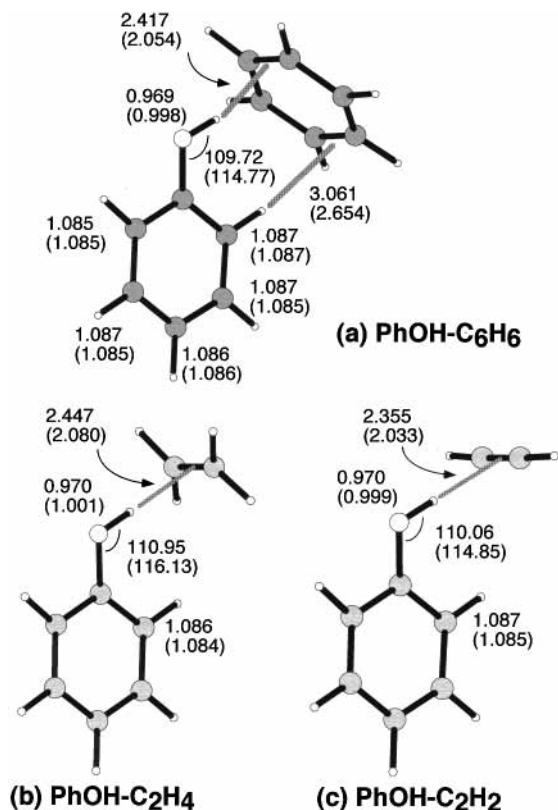


**Figure 2.** Energy optimized structures of (a) phenol–benzene, (b) phenol–ethylene, and (c) phenol–acetylene at the B3LYP/6-31G(d, p) level of calculations. Key structural parameters in the neutral ground state are shown in the figures. Values in the parentheses are structural parameters in the cationic ground state. The unit of the bond length is Å, and that of the angle is degree.

bonded to stabilize the cluster. This structure is the unique  $\pi$ -hydrogen-bonded structure for phenol–benzene found in the B3LYP/6-31G(d, p) level calculations. On the other hand, two stable  $\pi$ -hydrogen-bonded structures were found for phenol–ethylene. In the minimum energy structure, as seen in Figure 2, the hydroxyl group of the phenol moiety faces to the center of the CC double bond, and the ethylene moiety is perpendicular to the phenyl ring plane of phenol. When the ethylene moiety rotates around the  $\pi$ -hydrogen bond and locates in the same plane as the phenyl ring, it results in the other  $\pi$ -hydrogen-bonded isomer, which is estimated to be 0.30 kcal/mol higher in energy. The minimum energy structure of phenol–acetylene is similar to that of phenol–ethylene. The hydroxyl group is bound to the center of the CC triple bond, and the acetylene moiety is perpendicular to the phenyl ring plane. In the case of phenol–acetylene, only one  $\pi$ -hydrogen-bonded structure was obtained in the calculations; when the acetylene moiety is parallel to the phenyl ring plane, the hydrogen–hydrogen repulsion makes such a structure unstable.

The calculated OH stretching frequencies based on the minimum energy structures of the clusters are given in Figure 1, and are represented by bar graphs together with the observed spectra. A scaling factor of 0.9566 is determined to fit the observed OH frequency of bare phenol, and is applied to all the calculated frequencies. The calculated OH frequencies of the clusters well reproduce the observed values. This is a clear experimental support for the calculated  $\pi$ -hydrogen-bonded structures shown in Figure 2.

The DFT calculations for all the clusters predict essentially the same O–H bond length in the phenol moiety, as well as

the C–O–H angle, suggesting the similar  $\pi$ -hydrogen bond strength for all. This is consistent with the experimental results that the observed OH stretching frequencies of all the clusters are very similar. The distance between the H atom in the hydroxyl group and the CC bond of the acceptor site is around 2.4 Å. This is significantly longer compared to the proton-donor distance in the conventional  $\sigma$ -hydrogen bond (<2.0 Å).

As for phenol–ethylene, the other isomer cluster (+0.30 kcal/mol in energy) also gives almost the same OH vibrational frequency (+3  $\text{cm}^{-1}$ ) as that of the minimum energy structure. Though the presence of the  $\pi$ -hydrogen bond in the cluster is unequivocal, it is, at present, difficult to determine the conformation of the ethylene moiety relative to the phenyl ring because of the quite small difference in the energy and OH frequency between the two isomers.

The B3LYP/6-31G(d, p) level calculations estimate the binding energies of the  $\pi$ -hydrogen-bonded clusters to be 1.2, 1.4, and 1.9 kcal/mol for phenol–benzene, pheno–ethylene, and phenol–acetylene, respectively, including the zero-point energy (ZPE) and basis set superposition error (BSSE) corrections. The BSSE correction is done by the conventional counterpoise method.<sup>17</sup> The binding energy of phenol–benzene is experimentally estimated to lie in the range of 3.57–4.43 kcal/mol by the time-resolved photofragment detection study of Knee et al.<sup>10</sup> Because of the similar OH frequency shifts, the binding energies of phenol–ethylene and phenol–acetylene are also reasonably estimated to be around 4 kcal/mol. Though the calculated vibrational frequencies well reproduce the observed values, the B3LYP/6-31G(d, p) level calculations remarkably underestimate the binding energies of the  $\pi$ -hydrogen bonds. It has been pointed out that the B3LYP functional will inadequately account for dispersion forces. It is probably responsible for the underestimation of the binding energies.<sup>18,19</sup>

**3. The Proton Affinity and  $\pi$ -Hydrogen Bond Strength.** It is unexpected that the OH frequencies of these three  $\pi$ -hydrogen-bonded clusters are quite similar irrespective of the significant difference of the carbon–carbon multiple bonds in the acceptors, because the proton affinity of benzene (179.3 kcal/mol) is much larger than those of ethylene (162.6 kcal/mol) and acetylene (153.3 kcal/mol).<sup>20</sup> In the case of  $\sigma$ -hydrogen-bonded phenol–base (1:1) clusters, a good correlation between the proton affinity and the OH frequency shift has been known, as shown in Figure 3.<sup>13</sup> The similar plot of the phenol  $\pi$ -hydrogen-bonded clusters is also shown in Figure 3. Points for phenol–ethylene and –acetylene fall well on the extrapolated line of the correlation for the  $\sigma$ -hydrogen bond case, while pheno–benzene clearly deviates from the line. The similar peculiar behavior of phenol–benzene is also found in the relation between the proton affinity and the  $S_1$ – $S_0$  origin band shift. A good correlation between the proton affinity and the  $S_1$ – $S_0$  origin band shift is observed in the  $\sigma$ -hydrogen-bonded phenol clusters, as seen in the plot in Figure 4.<sup>21</sup> The points of the  $\pi$ -hydrogen-bonded phenol clusters are overlaid in Figure 4. Phenol–ethylene and –acetylene show the same correlation as that of the  $\sigma$ -hydrogen-bonded phenol clusters, however, phenol–benzene clearly deviates again from the line.

These two plots of the observed spectral shifts demonstrate that the proton affinity of the  $\pi$ -systems is a useful measure for the  $\pi$ -hydrogen bond strength as well as for the conventional  $\sigma$ -hydrogen bonds, though there is an exception in the case of phenol–benzene. For phenol–benzene, as seen in Section III.A.2, not only the O–H- -  $\pi$ -hydrogen bond but also a C–H- -  $\pi$ -hydrogen bond contributes to the most stable form. The optimization of the O–H- -  $\pi$ -hydrogen bond might be

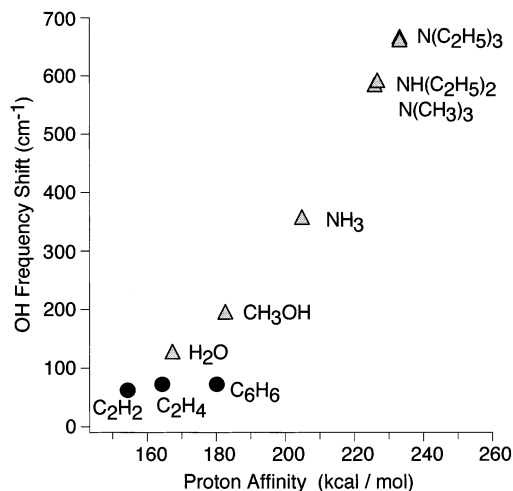


**Figure 3.** Low-frequency shifts of the OH stretching vibrational frequencies in the phenol-X clusters in  $S_0$  versus the proton affinities of the proton-acceptor molecules (X). The OH frequency shifts for X = C<sub>6</sub>H<sub>6</sub>, C<sub>2</sub>H<sub>4</sub>, and C<sub>2</sub>H<sub>2</sub> are obtained in this study. Those for X = H<sub>2</sub>O, CH<sub>3</sub>OH, NH<sub>3</sub>, N(CH<sub>3</sub>)<sub>3</sub>, NH(C<sub>2</sub>H<sub>5</sub>)<sub>2</sub>, and N(C<sub>2</sub>H<sub>5</sub>)<sub>3</sub> are taken from ref 13. The proton affinities are taken from ref 20.

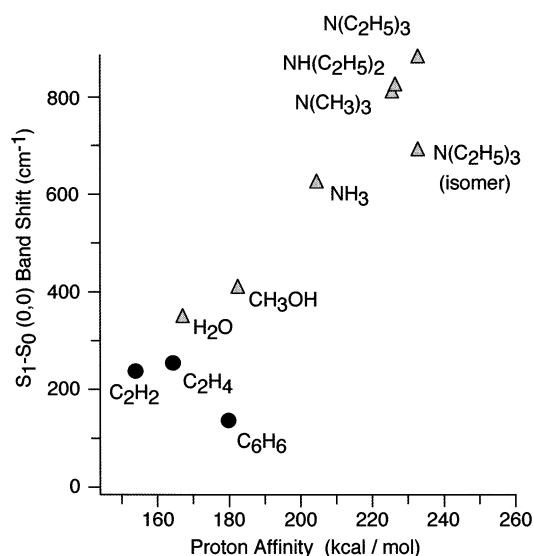


**Figure 4.** Low-frequency shifts of the  $S_1-S_0$  origin bands of the phenol-X clusters versus the proton affinities of the proton-acceptor molecules (X). The origin band shifts for X = C<sub>2</sub>H<sub>4</sub>, and C<sub>2</sub>H<sub>2</sub> are obtained in this study. Those for X = C<sub>6</sub>H<sub>6</sub> are taken from ref 8. Those for X = H<sub>2</sub>O, CH<sub>3</sub>OH, NH<sub>3</sub>, N(CH<sub>3</sub>)<sub>3</sub>, NH(C<sub>2</sub>H<sub>5</sub>)<sub>2</sub>, and N(C<sub>2</sub>H<sub>5</sub>)<sub>3</sub> are taken from ref 21. The proton affinities are taken from ref 20.

partly sacrificed by the C-H... $\pi$ -hydrogen bond formation, resulting in the smaller shifts of the OH frequency and the  $S_1-S_0$  origin band than expected from the correlation with respect to the proton affinity of benzene.

For 1-naphthol-benzene, which seems to be the system similar to the present clusters, in contrast, it has been suggested that the dispersive and inductive interactions are significant for the cluster formation.<sup>22</sup> Leutwyler and co-workers determined accurate intermolecular binding energies in the clusters of 1-naphthol with various base (proton acceptor) molecules in  $S_0$  by using the stimulated emission pumping resonance ionization technique, and found that the intermolecular binding energies of 1-naphthol-benzene and 1-naphthol-cyclohexane show a good correlation to the polarizability component parallel to the O-H bond ( $\alpha_{zz}$ ). Based on these facts, they suggested that the dispersive and inductive interactions are important for the cluster

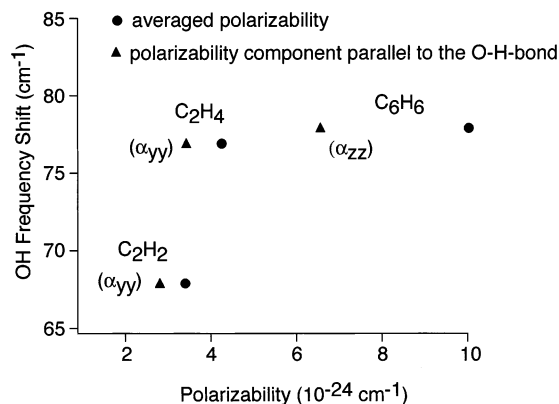


**Figure 5.** Low-frequency shifts of the OH stretching vibrational frequencies in the phenol-X clusters in  $S_0$  versus the averaged polarizabilities and parallel components of the polarizabilities of the proton-acceptor molecules (X). The OH frequency shifts for X = C<sub>6</sub>H<sub>6</sub>, C<sub>2</sub>H<sub>4</sub>, and C<sub>2</sub>H<sub>2</sub> are obtained in this study. The values of the polarizabilities are taken from refs 23-26.

formation between 1-naphthol and benzene, representing that 1-naphthol-benzene should be classified as a van der Waals cluster rather than a  $\pi$ -hydrogen-bonded cluster. In this respect, Figure 5 shows the plot of the OH frequency shift versus the polarizability (and its parallel component) of the acceptor of the present phenol clusters. The OH frequency shifts are poorly correlated with both averaged polarizability and its parallel component, suggesting that the dispersive and inductive terms are not necessarily dominant in the present  $\pi$ -hydrogen-bonded clusters.

**B.  $\pi$ -Hydrogen Bonds in the Cationic Ground State. 1. IR Spectra of the OH Stretching Vibrational Region.** Figure 6 shows the IR spectra of (a) bare phenol<sup>+</sup>, (b) (phenol-benzene)<sup>+</sup>, (c) (phenol-ethylene)<sup>+</sup>, and (d) (phenol-acetylene)<sup>+</sup> in the 3  $\mu$ m region. All the cations were produced by REMPI of the neutrals via the  $S_1$  vibrational ground state. The IRPD technique was utilized to observe the spectra of the cluster cations, while the IR spectrum of the bare phenol cation was measured by using another technique called autoionization-detected infrared (ADIR) spectroscopy. Details of ADIR spectroscopy and its application to the phenol cation were described elsewhere.<sup>27,28</sup> Here we only briefly describe its result. The OH band of the bare cation is found at 3534 cm<sup>-1</sup>, showing a low-frequency shift of 123 cm<sup>-1</sup> from the neutral band. This shift of the bare molecular cation is interpreted in terms of the enhancement of the double bond character of the C-O bond resulting in the O-H bond weakening upon ionization. On the other hand, the IR spectra of all the cluster cations show an extremely large change upon ionization, and their spectral features are quite similar with each other; an intense and broad band appears around 3050 cm<sup>-1</sup> in all the spectra. A weak and broad shoulder band is also seen at the high-frequency side of the intense band. The frequency differences between the major and shoulder bands are 160, 150, and 170 cm<sup>-1</sup> for (phenol-benzene)<sup>+</sup>, (phenol-ethylene)<sup>+</sup>, and (phenol-acetylene)<sup>+</sup>, respectively. In the case of (phenol-acetylene)<sup>+</sup>, a sharp peak centered at 3251 cm<sup>-1</sup> is overlapped on the shoulder band. No band is found above 3300 cm<sup>-1</sup> in all the spectra of the cluster cations.

The IR spectrum of (phenol-benzene)<sup>+</sup> has already been reported in a previous paper.<sup>11</sup> In the previous study, the cluster cation was produced by a pick-up type ion source; a bare phenol cation was first produced by resonant photoionization of phenol, then the cluster cation was formed by collisions with benzene and buffer He. The pick-up type cluster ion source favors the

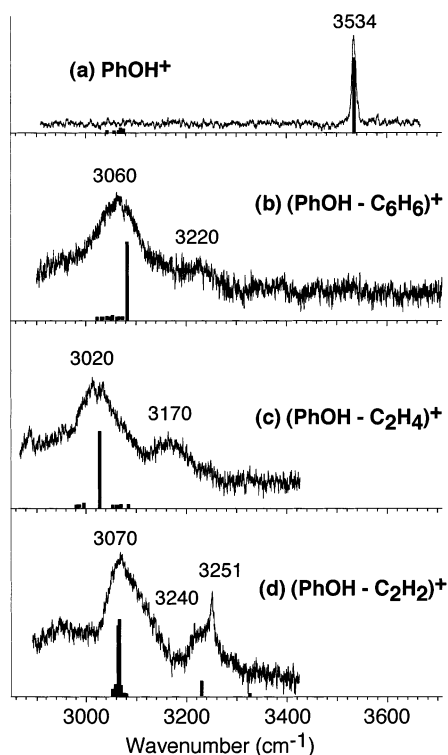


**Figure 6.** OH stretching vibrational region of IR spectra of (a) bare phenol, (b) phenol–benzene, (c) phenol–ethylene, and (d) phenol–acetylene in the cationic ground state ( $D_0$ ). The infrared photodissociation spectroscopy is used to record spectra (b)–(d), while autoionization-detected infrared spectroscopy is utilized to measure spectrum (a). Bar graphs below the observed spectra are the simulated IR spectra based on the energy-optimized structures at the B3LYP/6-31G(d, p) level. The scaling factor of 0.9492 is applied to all the calculated frequencies.

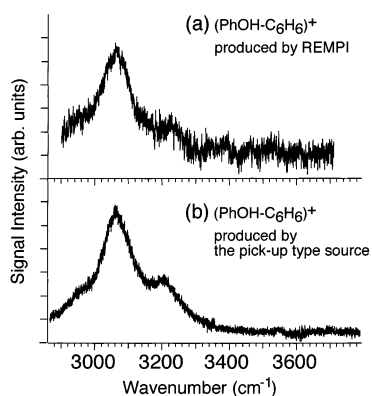


**Figure 7.** Comparison of the IR spectra of the (phenol–benzene)<sup>+</sup> cluster cation prepared by different methods: (a) (phenol–benzene)<sup>+</sup> produced by resonance enhanced multiphoton ionization of the neutral phenol–benzene cluster; (b) (phenol–benzene)<sup>+</sup> produced by the pick-up type ion source. See text.

production of the most stable cluster cation.<sup>29,30</sup> On the other hand, the structure of the cluster cation produced with REMPI of the neutral cluster reflects the Franck–Condon overlap between the cationic and neutral states. When the  $\pi$ -hydrogen-bonded cluster is photoionized, the production of the cluster cation having a  $\pi$ -hydrogen bond is expected because of the favorable Franck–Condon overlaps from the most stable form in the neutral state.

Figure 7 shows a comparison of the IR spectra of (phenol–benzene)<sup>+</sup> prepared by two different methods; (a) represents the spectrum for the REMPI produced cluster cation, which is

taken from Figure 6b, and (b) is one for the cation produced by the pick-up type source. These two spectra show the exactly same features, indicating that the  $\pi$ -hydrogen-bonded form is most stable also in the cation. The intense peak at  $3060\text{ cm}^{-1}$  in the IR spectra of the cluster cation is uniquely assigned to the band due to the  $\pi$ -hydrogen-bonded OH stretching vibration. As shown later, DFT calculations also support this assignment. In addition, the IR spectrum of the deuterated cluster cation,  $(\text{C}_6\text{D}_5\text{OH}-\text{C}_6\text{D}_6)^+$ , was reported by Inokuchi et al., and the same spectral features were observed, confirming that the contribution of aromatic CH stretching bands, which are also expected in this region, is negligible.<sup>31</sup> As seen in the IR spectrum of the bare phenol cation, CH stretching vibrational bands of aromatic cations are quite weak, and they are usually buried in the intense OH band.<sup>12,27</sup>

The similarity of these IR spectra indicates that all these cluster cations must have similar  $\pi$ -hydrogen-bonded structures, and that the phenolic OH vibration of the cluster cations exhibits an extremely large low-frequency shift of over  $450\text{ cm}^{-1}$  in comparison with the bare cation. The shifts are almost the same among the three cluster cations despite the different proton affinities of the acceptors. Though the hydrogen bonds in the cluster cations are of  $\pi$ -type, the OH shifts are as large as those found for the  $\sigma$ -hydrogen-bonded clusters of phenol with a strong base, such as phenol–ammonia ( $-363\text{ cm}^{-1}$ ) and –trimethylamine ( $-590\text{ cm}^{-1}$ ) in  $S_0$ .<sup>13</sup> Because the ionization potential of benzene ( $74556\text{ cm}^{-1}$ ),<sup>32</sup> ethylene, ( $84745\text{ cm}^{-1}$ ),<sup>23</sup> and acetylene ( $91952\text{ cm}^{-1}$ )<sup>33</sup> is substantially larger than that of phenol ( $68625\text{ cm}^{-1}$ ),<sup>34</sup> the positive charge in the cluster cations is approximately localized on the phenol moiety. The positively charged phenol moiety is known to greatly enhance its acidity, indicating strong electrostatic and inductive interactions.<sup>4,35</sup> The experimental results show a clear indication that the  $\pi$ -hydrogen bonds in the cluster cations are no longer categorized into a class of weak hydrogen bonds.

In all the IR spectra of the cluster cations, it is noticed that a shoulder band appears in the  $150\text{--}170\text{ cm}^{-1}$  high-frequency side of the OH stretching band. For this feature, there may be three possible cases: (1) a hydrogen-bonded OH stretching band of an isomer cluster cation, (2) a combination band involving an intermolecular vibration, and (3) an overtone band of the OH bending vibration. For case (1), we have examined the IR spectra obtained by using different methods for cluster cation preparation, as illustrated in Figure 7, as an example. If the shoulder band is due to another isomer cation, its relative intensity with respect to the major band is expected to be altered, because of different abundance associating the different production methods. However, the two spectra observed are essentially the same with each other, opposing the case. As for case (2), the difficulty arises from the fact that the frequency difference between the major and shoulder bands is almost unchanged, irrespective of large difference in masses of the proton acceptors (benzene, ethylene, and acetylene). As discussed later, these  $\pi$ -hydrogen-bonded cluster cations exhibit similar binding energies, leading to similar force constants of their intermolecular vibrations. In such a case, vibrational frequencies of their intermolecular modes substantially depend on their reduced mass. Case (3), the appearance of the OH bending overtone band borrowing the intensity from the neighboring OH stretching vibration, therefore, is the most feasible assignment for the shoulder band. The similar appearance of the OH bending overtone bands is known for hydrated anion clusters, in which hydrogen-bonded OH stretching vibrations are low-frequency shifted down to the  $3000\text{--}3200\text{ cm}^{-1}$  region.<sup>36</sup>

2. *DFT Calculations of the Cluster Cations.* DFT calculations of the bare phenol and the cluster cations were carried out at the B3LYP/6-31G(d, p) level. All the three cluster cations hold the  $\pi$ -hydrogen-bonded structures, and their minimum energy structures are very similar to those in the neutral ground state shown in Figure 2. In the case of (phenol-benzene)<sup>+</sup>, the  $\pi$ -hydrogen bond is localized on one of CC bonds of the benzene moiety, and a CH bond of the phenol moiety forms another  $\pi$ -hydrogen bond with the benzene moiety. In (phenol-ethylene)<sup>+</sup> and (phenol-acetylene)<sup>+</sup>, the hydroxyl group of the phenol moiety points the center of the CC multiple bond of the acceptor moiety.

The key structural parameters of the cationic ground state are given in parentheses in Figure 2. The O-H bond length and C-O-H angle in the phenol moiety are evaluated to be essentially the same among all the three  $\pi$ -hydrogen-bonded cluster cations, suggesting that the hydrogen bond form should be essentially determined by a local interaction between the hydroxyl group of the donor site and the  $\pi$ -electron(s) of the CC bond of the acceptors. Upon the ionization, it is noticed that the OH bond lengths become longer than those of neutrals, while the intermolecular distances are substantially reduced in accord with the enhancement of the  $\pi$ -hydrogen bond in the cationic state. The reduction of the intermolecular distance is more significant ( $\approx 15\%$ ) than the increase of the OH bond length ( $\approx 3\%$ ). As it has been known, the C-H bond lengths of substituted benzenes slightly decrease in their cationic state, resulting in the high-frequency shifts of the aromatic C-H stretching vibration(s) upon ionization.<sup>12,37</sup> For all the cluster cations, C-H bond lengths exhibit the same tendency. In (phenol-benzene)<sup>+</sup>, only the C-H bond of the phenol site bound to the benzene site shows a slightly longer bond length than the other C-H bonds. This is attributed to the extra C-H  $\pi$ -hydrogen bond formation, whose effect on the C-H bond is hardly seen in the neutral cluster.

The expected IR bands based on the minimum energy structures at the B3LYP/6-31G(d, p) level are indicated as bar graphs in the observed spectra in Figure 6. All the calculated frequencies are scaled by a factor of 0.9492, which is determined for the OH stretching vibrational frequency of the bare phenol cation to be reproduced. The simulated IR spectra well reproduce the observed spectra of the cluster cations, confirming the above assignment of the intense band as their  $\pi$ -hydrogen-bonded OH stretching vibration. The CH stretching vibrations of the aromatic CH both in the phenol and benzene moieties are also expected to appear in this region. Their intensities, however, are estimated to be much less than that of the OH stretching vibration, and they would be buried in the intense OH stretch band. In the case of (phenol-benzene)<sup>+</sup> and (phenol-ethylene)<sup>+</sup>, the OH stretching vibration is well isolated from the aromatic CH stretching vibration of the phenol moiety, while those modes are found to be extensively mixed in (phenol-acetylene)<sup>+</sup>. In the latter case, actually, the simulation reveals that the intensity of the OH stretching vibrations is distributed to several bands in the 3000–3100 cm<sup>-1</sup>. However, it is difficult to confirm this mode mixing in the observed spectrum because of such a band broadening. The simulated IR spectra fail to reproduce the shoulder of the OH stretch band. This is because the harmonic approximation is included in the spectral simulation, and no overtone and combination bands can be simulated. In the case of (phenol-acetylene)<sup>+</sup>, a band of the moderate intensity is predicted at 3228 cm<sup>-1</sup>. This is the antisymmetric CH stretching vibration of the acetylene moiety, and it corresponds to the sharp band at 3251 cm<sup>-1</sup> in the observed spectrum.

This CH stretch band is overlapped with the OH bending overtone band in the observed spectrum.

3. *The  $\pi$ -Hydrogen Bond Energies in the Cluster Cations.* The OH frequency shifts of the  $\pi$ -hydrogen-bonded cluster cations are substantially larger than that for phenol-water ( $-133$  cm<sup>-1</sup>) clusters in S<sub>0</sub>, which is a typical  $\sigma$ -hydrogen-bonded clusters.<sup>4,13</sup> This suggests that the  $\pi$ -hydrogen bond strength in the cations is stronger than  $\sigma$ -hydrogen bonds of phenol with typical base molecules in S<sub>0</sub>. The hydrogen bond energy of phenol-water in S<sub>0</sub> is precisely determined to be 5.478 kcal/mol based on the origin band shift of the S<sub>1</sub>-S<sub>0</sub> transition and the dissociation energy in D<sub>0</sub>.<sup>38</sup> Therefore, it is safely stated that the  $\pi$ -hydrogen bond energy of these cluster cations is larger than 5–6 kcal/mol.

Another estimation of the lower limit of the  $\pi$ -hydrogen bond strength can be carried out for (phenol-benzene)<sup>+</sup> by considering a comparison with the charge resonance (CR) interaction in the cluster cation. If (phenol-benzene)<sup>+</sup> had a sandwich-type form consisting of a parallel pair of the aromatic rings, similar to the benzene dimer cation, the binding energy of the cluster cation would be given by the CR interaction.<sup>39</sup> The binding energy due to the CR interaction ( $\Delta E_{\text{CR}}$ ) is given by

$$\Delta E_{\text{CR}} = -\frac{\Delta\text{IP}}{2} + \frac{1}{2}\{(\Delta\text{IP})^2 + 4\epsilon^2\}^{1/2} \quad (1)$$

where  $\Delta\text{IP}$  is the difference of the ionization potentials between two components of the dimer, and  $\epsilon$  is the CR interaction matrix element. For phenol-benzene,  $\Delta\text{IP}$  is 0.735 eV, and  $\epsilon$  is 0.67 eV if we assume the same value as the benzene dimer cation.<sup>40</sup> Then,  $\Delta E_{\text{CR}}$  is roughly estimated to be 0.4 eV ( $\approx 9$  kcal/mol). On the other hand, however, it was reported that (phenol-benzene)<sup>+</sup> shows no strong CR absorption in the near-infrared region, representing a structure other than the parallel sandwich type.<sup>41</sup> This result indicates that the  $\pi$ -hydrogen bond energy is dominant over the CR interaction,  $\Delta E_{\text{CR}}$ . It is, therefore, concluded that the  $\pi$ -hydrogen bond strength in (phenol-benzene)<sup>+</sup> is larger than the expected CR stabilization energy, 0.4 eV ( $\approx 9$  kcal/mol). This result is consistent with the above estimation based on the OH frequency shift. Because (phenol-ethylene)<sup>+</sup> and (phenol-acetylene)<sup>+</sup> show OH stretching frequencies very similar to that of (phenol-benzene)<sup>+</sup>, the binding energies of these cluster cations are also roughly estimated to be larger than 9 kcal/mol.

The binding energy of phenol-benzene in the neutral ground state was experimentally determined to be in the range of 3.57–4.43 kcal/mol by the time-resolved photofragment detection study.<sup>10</sup> The above estimation suggests that the  $\pi$ -hydrogen bond strength becomes at least twice stronger upon the ionization. It has been found for several  $\sigma$ -hydrogen-bonded clusters that hydrogen bond strength doubles or triples upon ionization.<sup>35</sup> The present results represent a general trend for  $\pi$ -hydrogen-bonded clusters in the neutral cationic states.

At the B3LYP/6-31G(d, p) level calculations, the intermolecular binding energies based on the minimum energy structures are evaluated to be 12.0, 9.1, and 10.1 kcal/mol for (phenol-benzene)<sup>+</sup>, (phenol-ethylene)<sup>+</sup>, and (phenol-acetylene)<sup>+</sup>, respectively, including the BSSE and ZPE corrections. These calculated binding energies are 5–10 times larger than those of the neutral ground state. This result qualitatively supports the remarkable enhancement of the  $\pi$ -hydrogen bond strength, and is consistent with the above estimation of the lower limit of the binding energy based on the experimental results. Though the reliability of this level of calculations is somewhat questionable for the aim of the precise estimation of the binding

energy, as seen in the neutral ground state, electrostatic terms become more important in the case of the cluster cation and it might make the energy calculations more reliable.

#### IV. Summary

In this study, we reported the IR spectra of phenol–benzene, –ethylene, and –acetylene in the OH stretching vibrational region. In the neutral ground state, the OH stretching vibration of the phenol site of the clusters showed characteristic low-frequency shifts due to the  $\pi$ -hydrogen bond formation. The OH frequency shifts did not remarkably depend on the source of the  $\pi$ -electrons, aromatic ring, double bond, nor triple bond. The  $\pi$ -hydrogen-bonded structures were also supported by theoretical calculations at the B3LYP/6-31G(d, p) level, and the observed IR spectra were well reproduced based on the minimum energy structures at this calculation level. In the case of phenol–benzene, not only the hydroxyl group but also the C–H bond of the phenol site forms a  $\pi$ -hydrogen bond with benzene. The OH frequency shifts are smaller than those in the conventional  $\sigma$ -type hydrogen bonds, indicating weaker strength of the  $\pi$ -hydrogen bond. Phenol–benzene showed the much smaller OH frequency shift than that expected from the proton affinity of benzene, while the OH shifts of phenol–ethylene and –acetylene fell on the correlation line extrapolated from the data on the  $\sigma$ -type hydrogen-bonded phenol clusters. The  $S_1$ – $S_0$  origin band shifts of these three  $\pi$ -hydrogen-bonded clusters also showed the similar tendency. It was suggested that the C–H– $\pi$ -hydrogen bond in phenol–benzene might be the origin of the anomaly. Phenol–benzene, –ethylene, and –acetylene hold the  $\pi$ -hydrogen-bonded structures upon the ionization. However, the OH frequency shifts due to the  $\pi$ -hydrogen bond significantly increased, indicating the drastic enhancement of the  $\pi$ -hydrogen bond strength upon the ionization. Based on the comparison between the IR spectra of (phenol–benzene)<sup>+</sup> produced by REMPI and the pick-up type ion source, it was confirmed that the  $\pi$ -hydrogen-bonded structure is the most stable structure of the cluster cation. The DFT calculations also well reproduced the observed large OH frequency shifts, supporting the  $\pi$ -hydrogen-bonded structures of the cations. The lower limit of the  $\pi$ -hydrogen bond energies of the cluster cations was roughly estimated to be 9 kcal/mol based on the OH frequency shifts and missing of the CR band.

**Note Added in Proof.** After we submitted the paper, a paper on theoretical calculations of (phenol–benzene)<sup>+</sup> was published.<sup>42</sup> This work also supported the  $\pi$ -hydrogen-bonded structure of the cluster cation.

**Acknowledgment.** The authors acknowledge Ms. K. Nagao for her contribution in the early stage of this work. We are grateful to Dr. H. Ishikawa, Dr. T. Maeyama, Dr. N. G. Patwari, and Mr. M. Kayano for helpful discussion.

#### References and Notes

- (1) Pimentel, G. E.; McClellan, A. L. *The Hydrogen Bond*, W. H. Freeman and Company, San Francisco, **1960**.
- (2) Jeffrey, G. A. *An Introduction to Hydrogen Bonding*, Oxford University Press: New York, **1997**.
- (3) Zwier, T. S. *Ann. Rev. Phys. Chem.* **1996**, *47*, 205.
- (4) Ebata, T.; Fujii, A.; Mikami, N. *Int. Rev. Phys. Chem.* **1998**, *17*, 331.
- (5) Brutschy, B. *Chem. Rev.* **2000**, *100*, 3891.
- (6) Oikawa, A.; Abe, H.; Mikami, N.; Ito, M. *J. Phys. Chem.* **1983**, *87*, 5083.
- (7) Fujii, A.; Patwari, N. G.; Ebata, T.; Mikami, N. *Int. J. Mass Spectrometry*, in press.
- (8) Abe, H.; Mikami, N.; Ito, M. *J. Phys. Chem.* **1982**, *86*, 1768.
- (9) Hartland, G. V.; Henson, B. F.; Venturo, V. A.; Felker, P. M. *J. Phys. Chem.* **1992**, *96*, 1164.
- (10) Knee, J. L.; Khunder, L. R.; Zweil, A. H. *J. Chem. Phys.* **1987**, *87*, 115.
- (11) Fujii, A.; Iwasaki, A.; Yoshida, K.; Ebata, T.; Mikami, N. *J. Phys. Chem. A* **1997**, *101*, 1798.
- (12) Fujii, A.; Fujimaki, E.; Ebata, T.; Mikami, N. *J. Chem. Phys.* **2000**, *112*, 6275.
- (13) Iwasaki, A.; Fujii, A.; Ebata, T.; Mikami, N. *J. Phys. Chem.* **1996**, *100*, 16053.
- (14) Frisch, M. J.; Trucks, G. W.; Schlegel, H. B.; Scuseria, G. E.; Robb, J. M. A.; Cheeseman, R.; Zakrzewski, V. G.; Montgomery, J. A., Jr.; Stratmann, R. E.; Burant, J. C.; Dapprich, S.; Millam, J. M.; Daniels, A. D.; Kudin, K. N.; Strain, M. C.; Farkas, O.; Tomasi, J.; Barone, V.; Cossi, M.; Cammi, R.; Mennucci, B.; Pomelli, C.; Adamo, C.; Clifford, S.; Ochterski, J.; Petersson, G. A.; Ayala, P. Y.; Cui, Q.; Morokuma, K.; Malick, D. K.; Rabuck, A. D.; Raghavachari, K.; Foresman, J. B.; Cioslowski, J.; Ortiz, J. V.; Baboul, A. G.; Stefanov, B. B.; Liu, G.; Liashenko, A.; Piskorz, P.; Komaromi, I.; Gomperts, R.; Martin, R. L.; Fox, D. J.; Keith, T.; Al-Laham, M. A.; Peng, C. Y.; Nanayakkara, A.; Gonzalez, C.; Challacombe, M.; Gill, P. M. W.; Johnson, B.; Chen, W.; Wong, M. W.; Andres, J. L.; Gonzalez, C.; Head-Gordon, M.; Replogle, E. S.; and Pople, J. A. *Gaussian 98*, Revision A.7, Gaussian, Inc.: Pittsburgh, PA, **1998**.
- (15) Stevens, P. J.; Devlin, F. J.; Chablowski, C. F.; Frisch, M. J. *J. Phys. Chem.* **1994**, *98*, 11623.
- (16) These calculated structures are visualized by using *MOLCAT*, ver.2.5.2: Tsutui, Y.; Wasada, H. *Chem. Lett.* **1995**, 517.
- (17) Boys, F.; Bernardi, F. *Mol. Phys.* **1970**, *19*, 553.
- (18) Hobza, P.; J. Sponer, J.; Reschel, T. *J. Comput. Chem.* **1995**, *16*, 1315.
- (19) Chapman, D. M.; Müller-Dethlefs, K.; Peel, J. B. *J. Chem. Phys.* **1995**, *111*, 1955.
- (20) Hunter, E. L.; Lias, S. G. *J. Phys. Chem. Ref. Data* **1998**, *27*, 413.
- (21) Jouvét, C.; Lardeux-Dedonder, C.; Richard-Viard, M.; Solgadi, D.; Tramer, A. *J. Phys. Chem.* **1990**, *94*, 5041.
- (22) Wickleder, C.; Droz, T.; Bürgi, T.; Leutwyler, S. *Chem. Phys. Lett.* **1997**, *264*, 257.
- (23) *CRC Handbook of Chemistry and Physics*, 76th. Edition, Lide, D. R., Ed.; CRC Press: Boca Ration, **1995**.
- (24) Alms, G. R.; Burnham, A. K.; Flygare, W. H. *J. Chem. Phys.* **1975**, *63*, 3321.
- (25) Hills, G. W.; Jones, W. J. *Faraday Trans. II* **1975**, *71*, 812.
- (26) Amos, R. D.; Williams, J. H. *Chem. Phys. Lett.* **1979**, *66*, 471.
- (27) Fujii, A.; Iwasaki, A.; Ebata, T.; Mikami, N. *J. Phys. Chem. A* **1997**, *101*, 5963.
- (28) Fujimaki, E.; Fujii, A.; Ebata, T.; Mikami, N. *J. Chem. Phys.* **1999**, *110*, 4238.
- (29) Solcà, N.; Dopfer, O. *Chem. Phys. Lett.* **2000**, *325*, 354.
- (30) Solcà, N.; Dopfer, O. *J. Phys. Chem. A* **2001**, *105*, 5637.
- (31) Inokuchi, Y.; Nishi, N. *Ann. Rev. of Institute for Molecular Science* **1999**, *66*.
- (32) Fischer, I.; Linder, R.; Müller-Dethlefs, K. *J. Chem. Soc. Faraday Trans.* **1994**, *90*, 2425.
- (33) Pratt, S. T.; Dehmer, P. M.; Dehmer, J. L. *J. Chem. Phys.* **1993**, *99*, 6233.
- (34) Dopfer, O.; Müller-Dethlefs, K. *J. Chem. Phys.* **1994**, *101*, 8508.
- (35) Mikami, N.; Okabe, A.; Suzuki, I. *J. Phys. Chem.* **1988**, *92*, 1858.
- (36) Ayotte, P.; Weddle, G. H.; Kim, J.; Johnson, M. A. *J. Am. Chem. Soc.* **1998**, *120*, 12361.
- (37) Dopfer, O.; Olkhov, R. V.; Maier, J. P. *J. Chem. Phys.* **1999**, *111*, 10754.
- (38) Braun, J. E.; Mehnert, Th.; Neusser, H. J. *Int. J. Mass Spectrometry* **2000**, *203*, 1.
- (39) Ohashi, K.; Izutsu, H.; Inokuchi, Y.; Hino, K.; Nishi, N.; Sekiya, H. *Chem. Phys. Lett.* **2000**, *321*, 406.
- (40) Ohashi, K.; Nishi, N. *J. Phys. Chem.* **1992**, *96*, 2931.
- (41) Ohashi, K.; Nakae, Y.; Inokuchi, Y.; Nakai, Y.; Nishi, N. *Chem. Phys. Lett.* **1998**, *239*, 429.
- (42) Pejov, L. *Chem. Phys. Lett.* **2002**, *358*, 368.